www.czasopisma.pan.pl PAN POLSKA AKADEMIA NAUK www.journals.pan.pl

Arch. Min. Sci. **65** (2020), 3, 531-550

Electronic version (in color) of this paper is available: http://mining.archives.pl

DOI 10.24425/ams.2020.134133

MAREK ROTKEGEL[1], ŁUKASZ SZOT[1*], SŁAWOMIR FABICH[2]

THE ANALYSIS OF SELECTED METHODS OF THE YIELDING OF A CIRCULAR ARCH SUPPORT MADE OF V PROFILES

Steel yielding arch support constructed of V profiles is commonly used to protect galleries and, in some cases, to reinforce or secure a shaft support. For this purpose, a closed, circular-shaped arch support is used, with arches overlapped by clamps that are typical for this type of construction. The support has high resistance to the impact of even (distributed over the entire surface of the support) load, however, as a result of significant deformation associated with a change in the radius of the curvatures, the support shows limited yielding capacity. This is due to the increase in resistance to slide on the locks, resulting from changes in the geometry of the ring caused by the rock mass. This article presents the results of research and analysis concerning the elements of the arch support with notches in arches. The research team tested the effect of the depth and location of the notches of the section's flanges on the load impacting on the clamp's bolts and the strength of the roof support. Moreover, the tests covered the influence of the number and location of clamps in a frictional joint on the change in the nature of work and yielding capacity. Finally, the research included both strength tests of the support's elements, as well as strength analyses based on the finite element method.

Keywords: shaft, circular support, arch support

1. Introduction

A steel arch support, made of V-profiles, is the primary element designed to protect galleries in an underground mine. It is used in Polish hard coal mines and in mines in such countries as Ukraine, Russia, Turkey, China and Vietnam [1-6]. In some cases, it is also used to strengthen or protect the shaft support. Rings made of C-section profiles with bolted joints are commonly used for it [19]. It is also possible to use arches made of profiles which are overlapped with clamps

[1] CENTRAL MINING INSTITUTE, 1 GWARKÓW SQ., 40-166 KATOWICE, POLAND
[2] KGHM CUPRUM, WROCŁAW, POLAND

* Corresponding author: l.szot@gig.eu

typical for the construction of the arch support. Such support is resistant to various kinds of loads, especially those evenly distributed over the entire perimeter. However, under significant load deformation it has some disadvantages, due to the change in yielding capacity as the deformation progresses [18,20,22]. The purpose of the research and analysis described above was to improve the functionality of such support when it is used to secure a section of salt deposit of one of the copper ore mine shafts in Poland.

Rock salt is a rock with rheological properties, as a result of which, under the influence of the stresses occurring in the rock mass, it moves towards an excavation. The speed of this movement depends on many factors, of which the most important are:

- the amount of stress in the rock mass,
- the properties of the viscosity of the rock,
- the temperature and humidity of the rock and the environment.

The effect of the rheological flow of salt rock into the workings is the reduction of its cross-section. When the specific shear thickening threshold is exceeded, the salt rock pieces come loose from the salt rock and can fall into the shaft excavation.

2. Subject of the research

The analysed shaft is located in an area of the deposit where there is a layer of rock salt with a thickness of approximately 156 m, deposited in the depth range from 1026 to 1182 m. The shaft has a diameter of 7.5 m with a tube support as the basic support of the shaft (in the zone subjected to freezing), and with a concrete support below. The section of the shaft excavated in rock salt is lined with layer support reinforced with steel rings made of V25 profiles, built in spacing of 0.75 m (Fig. 1), combined with 10 segments connected by double shackle hooks

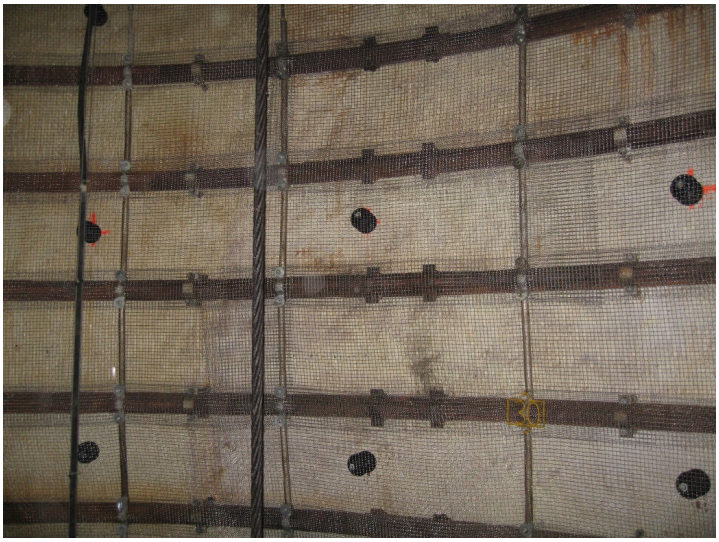

Fig. 1. The support protecting the shaft excavation over the salt deposit section

in SD-type. Each of the ring segments is fastened to the salt layer with a U-V25-24 grips for secondary bolting and anchored with two anchor hex bolts with a 1.8 m long rod. The support is covered with a layer of corrosion-resistant steel mesh applied to protect the shaft excavation in case of damage to any of the steel elements of the support.

The support built in the shaft has two functions. The first and primary one is to protect the shaft excavation against the possible consequences of the dilatation of salt rock, i.e. the destruction of the salt sidewall. This may cause a fragment of rock to fall into the shaft. The second function is to insulate the salt excavation from water and air flowing through the shaft.

Although the creep process was an expected phenomenon, the scale of the rheological processes in the initial period after the shaft excavation exceeded the expected values. In the case of this shaft, the dynamic parameters of this process were surprising. In the period immediately after the completion of the shaft, the creep was observed with a temporary speed of up to several mm/day. For example, at the measuring point with the highest speed of flow, built at the depth of 1084.5 m, the highest speed of the creep of the salt sidewall slightly exceeded 11.0 mm/day (double-sided creep) 17 days after the development of the excavation; this speed gradually reduced with time to reach the value of ~1.9 mm/day after 15 m (Fig. 2).

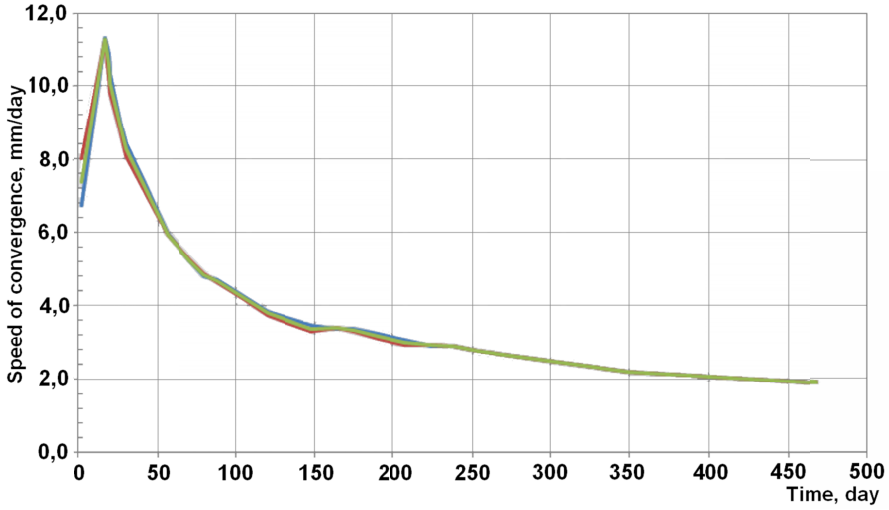

Fig. 2. Process of the two-sided creep of the shaft's salt sidewall – level 1084.5 m

The dynamics of the rock salt creep process did not change significantly after the first shaft redevelopment. Figure 3 shows the dynamics of the process of rock salt creep at the measuring station, i.e. after the redevelopment of the shaft, and presents a comparison of the results with the dynamics of the process before the redevelopment. The comparison indicates that immediately after the redevelopment of the salt section, the creep accelerated by about 50% compared to the one observed immediately before the redevelopment.

Immediately after the redevelopment of the salt section of the shaft, an increase in the dynamics of the movement of the salt mass to the excavation was observed at all measuring points. The graph presented in Fig. 4. shows that the highest displacements of 2÷2.75 mm/day

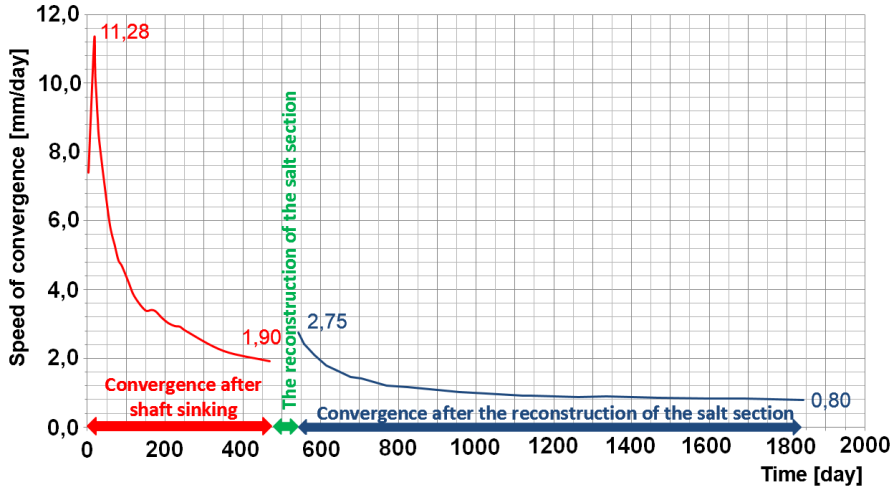

Fig. 3. Process of the double-sided creep of the salt shaft, recorded at station no. 2 – level 1084.5 m before and after the redevelopment of the shaft

were registered in the middle part of the salt layer. The convergence in the area of the roof and floor of the salt layer was lower, between 0.5 and 1.0 mm/day. Over time, the convergence speed decreased, reaching an average speed of 0.8 mm/day in the central part of the salt layer, to a value of below 0.5 mm/day in the area of its roof and floor. The convergence is still being observed.

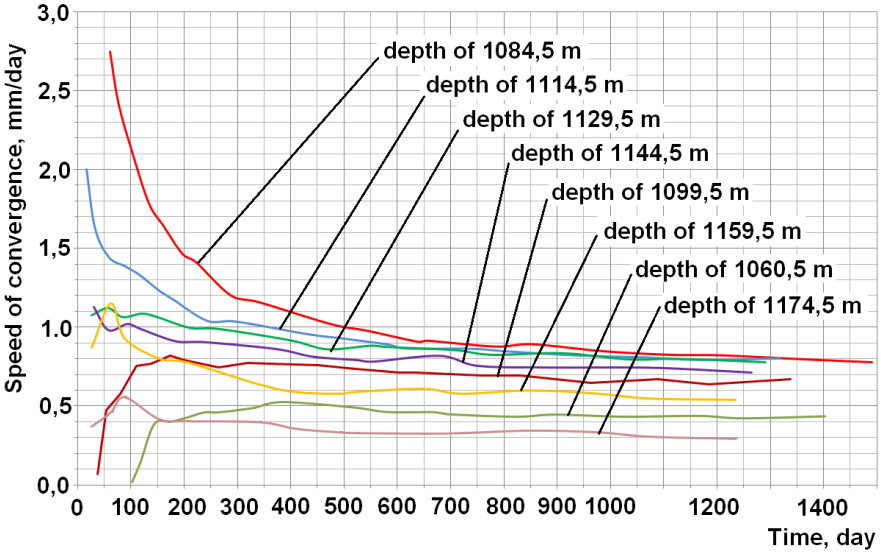

Fig. 4. Process of the double-sided creep of the shaft's saline sidewall, recorded at all measuring points between 25 June 2015 and 28 April 2019

The reinforcement of the base structure of the support, used during the first redevelopment of the salt section, did not significantly improve the performance characteristics of the steel support. The increase in the speed of deformation and length decreasing and stabilizing of this speed in comparison to this from before redevelopment caused some unfavourable changes in the support. By December 2016, which was one year after the completion of the salt segment redevelopment, a progressive process of damage to the pipe struts, breaking off of the bolts of the locks and breaking off of the fixing anchors through the U-V25-24 individual segments of the steel ring were registered.

It was noticed that the ever-increasing convergence of the salt excavation was intensifying. This meant there was a need to find or develop a way to increase the yielding capacity of the steel yielding support so that it could reduce its diameter as much as possible, by means of sliding-sections within the locks, with a reduction in the number of cases of the breaking off of U-bolts, as well as the breaking off of the anchors fixing the steel rings to the salt excavation. This article presents further results of laboratory tests and numerical simulations aimed at analysing the effects of actions which were implemented to improve the yielding capacity of the support.

3. Characteristics of a circular arch support

A circular arch support is rarely used in the galleries of Polish mines and is mainly used in cases of versatile loads. It is more widely used in Slovak mines [7]. Due to the circular contour of installation, it seems to be reasonable to use it as an element of shaft support or its reinforcement. An example of the use of circular arch support in horizontal excavations in Slovak mines is shown in Figure 5. Figures 6 to 7 present typical damages to this type of support when subjected to significant deformation loads.

Fig. 5. A circular support used in Slovakia

Fig. 6. Roof arch fracture

Fig. 7. Buckled roof arches

Circular arch supports were used as a basic element of the SW-4 shaft support in O/ZG Polkowice-Sieroszowice in the section of the rock salt layer. The arch support consists of 10 arches made of a V25 profile [8] rolled from S480W steel [9]. The length of the arches is L = 3700 mm and the radius of the curvature which is calculated to the bottom of the section is approximately R = 4800 mm. The arches are connected by an overlap of about 550 mm by means of SDS25 clamps (two clamps in each overlap).

The analysis of the geometry of the arch support by means of the RECOVERIES program enabled the more precise specification of the dimensions of the individual elements in order to obtain an arch support with an internal diameter that is equal to the diameters of the design (~9750 mm). With an arch length of L = 3700 mm the bending radius of the arches should be R = 4870 mm and the overlap c = 610 mm.

The yielding capacity of circular arch support is not only related to the load capacity of friction joints, the deformability of the arches is also an important factor. Change in diameter is related to two mechanisms that must occur simultaneously, i.e. slide in the friction joints (reduction of the circumference of the arch supports) and the simultaneous deformation of the arches (change of the radius of curvature). Assuming that all arches are deformed uniformly and the overlaps increase evenly, a 100 mm reduction in the diameter of the arch support is theoretically equal to a 50 mm change in the bending radius of the arches and a 30 mm increase in each overlap. In reality, the change in the radius of curvature must be greater, since it will not occur along the entire length of the arches, but only outside the friction joints, which are stiffer due to the combination of two sections. Such a change of geometry is associated with additional loads that act on the arches of the arch supports in addition to loads from the rock mass. It should also be noted that the resistance of friction joints (the axial forces transmitted by them) depends on the bending moment at the overlap.

The stress state of the sensitive areas of the arch supports was estimated using numerical analysis based on the finite element method [10,11] and calculated with the COSMOS/M program [12,13].

3.1. Numerical analysis of circular arch support bending

The first stage of the analysis included a test and the mapping of the behaviour of the arches subjected to bending. The material was bent so that mapped to radius of curvature changed by 50, 100, 150 and 200 mm. Firstly, it was determined which arch deflections corresponded to the individual radius changes. For a section of the arch, excluding overlaps, of length L=2480 mm, changes in the radius of curvature can be approximated as:

- radius change of 50 mm – arch deflection of 1.67 mm,
- radius change of 100 mm – arch deflection of 3.39 mm,
- radius change of 150 mm – arch deflection of 5.14 mm,
- radius change of 200 mm – arch deflection of 6.93 mm.

In the next step numerical model reflecting the geometry of one half of the arch was built [14,15]. The plane of symmetry was determined by the axes of symmetry of the section of the profiles. At this level, appropriate nodes were established. It consists of less than 15 thousand solid-type elements, described in a similar number of nodes. In addition, elastic elements were adopted at the support points to avoid stress concentrations resulting from the point and stiff support. The arch model was supported at the end of the overlaps and a continuous load acting on the bottom of the section was assumed. This being the test load, which is related to the bend of the arch to achieve a new, smaller radius of curvature, and not to the direct impact of the rock mass on the arch. Figures 9 and 10 show a model prepared for calculation and a fragment of the model with a visible representation of one half of the V25 profile.

In order to carry out comparative analysis of the work of different arch variants, three consecutive models were prepared. To simulate a section notch from the flange side, individual models had 30 mm, 40 mm and 50 mm deep notch.

Analysis was carried out for all four models, with the same support and load conditions to obtain a change in the curvature of the arches. Due to the obtained values of reduced stress being less than the yield strength of S480W steel, the simulations were performed in a linear range. The result of the calculations provided the deformation of the models, the values of support re-

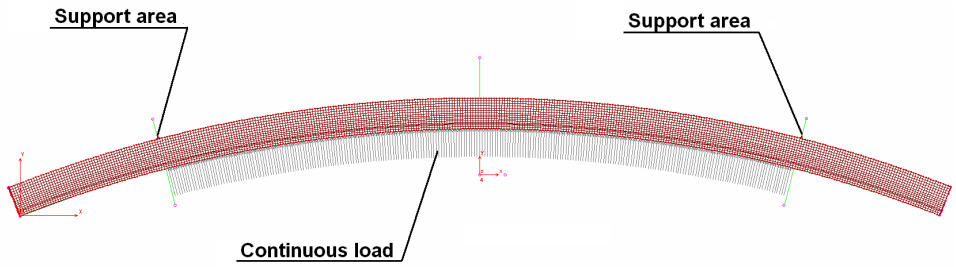

Fig. 9. Arch model prepared for calculation

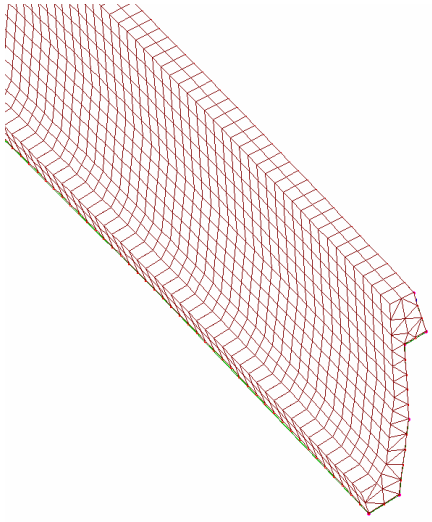

Fig. 10. Fragment of the model with a visible representation of the outline of the profile

actions and the values of internal forces that were automatically converted by the program into reduced stresses, according to the Huber-Misses hypothesis. The obtained results were also used to determine the force value required to change the geometry of the arch – reduction of the radius of curvature by 50, 100, 150 and 200 mm. Figures 14 and 17 show the distribution of stress in the X and Y directions. Additionally, Figure 18 shows the reduced stress distribution around the notch. The results of the analyses are presented in Table 1.

The results of the analysis indicate that a notch in the V25 profile, depending on its size, reduces the value of the force required to change the radius of the curvature of the arch from 14% (with a 30 mm notch) to 26% (with a 50 mm notch). At the same time, the reduced stress values increase by up to four times. In addition, when cutting to a depth of 50 mm and changing the radius of the curvature by 200 mm, the value of the reduced stresses may come close to the yield point of the material (steel S480W). In the actual system, however, the values of these stresses will be lower due to the presence of a compressive axial force in the arch, which is not included in these analyses.

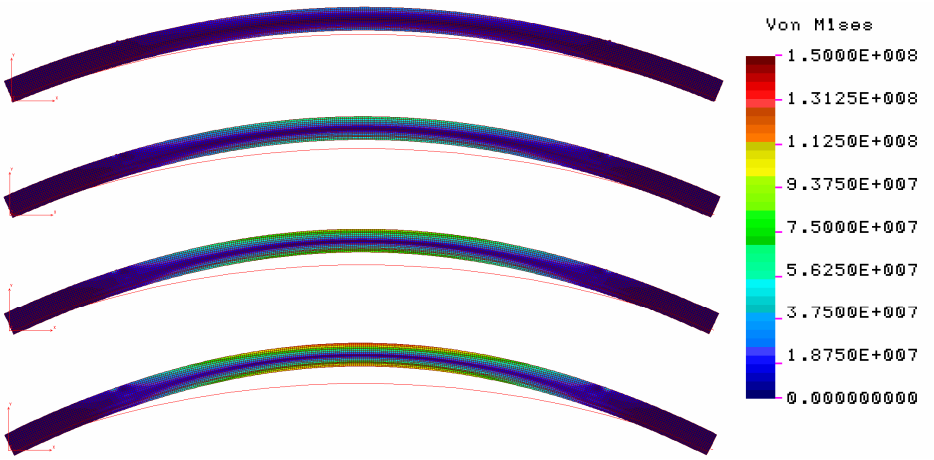

Fig. 14. Reduced stress distribution in the model of the arch without a notch for deformation corresponding to a radius reduction of 50, 100, 150 and 200 mm
(Stress in Pa, deformation scale 10×, red line – outline of the bottom of the non-deformed arch)

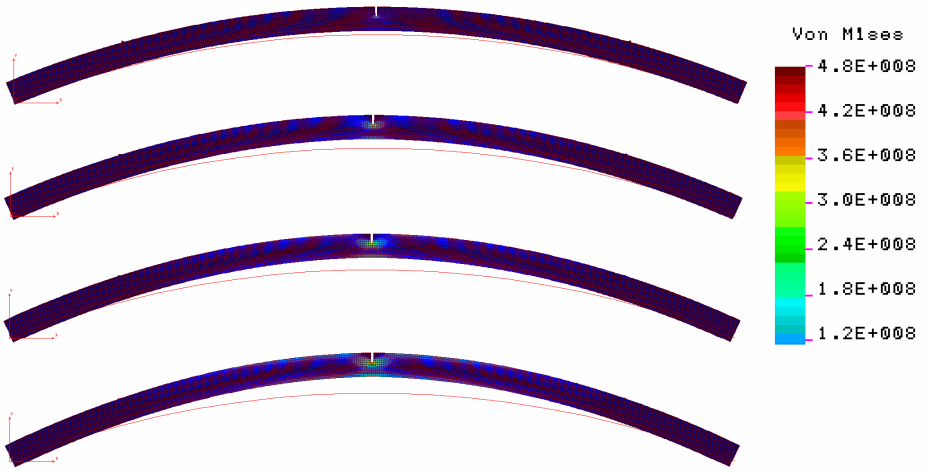

Fig. 17. Reduced stress distribution in the model of arches with a 50 mm notch for deformation corresponding to a radius reduction of 50, 100, 150 and 200 mm
(Stress in Pa, deformation scale 10×, red line – outline of the bottom of the non-deformed arch)

3.2. Numerical analysis of the bending of the frictional joint of circular arch support-notches on V25 profile flanges

In the second stage of the analysis, the slides in the friction joints of the support were modeled under increasing load. This enabled the determination of the effect of the change in the support's radius (due to deformation of the arches and slides) on the stress values in the V25 profile of the

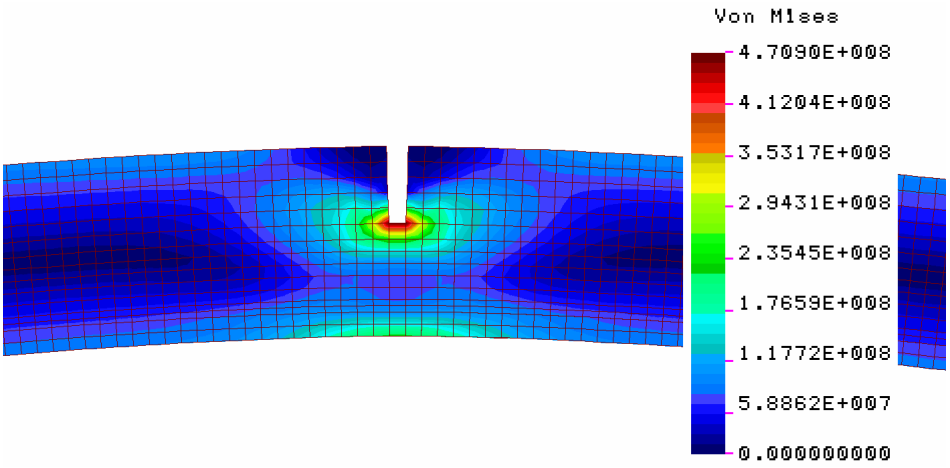

Fig. 18. The zoom of the arch section – reduced stress distribution in the model of an arch with a 50 mm notch for deformation corresponding to a radius reduction of 200 mm (stress in Pa, deformation scale 10×)

TABLE 1

Results of numerical analyses

Size of the arch notch	Radius change	Model deformation	Total load of model (F_V)	Average change of the load causing the radius change	Max. stress (von Mises)	Stress factor
mm			N	%	MPa	—
0	50	1,67	3666	100	30,2	1,0
	100	3,39	7901		65,1	1,0
	150	5,14	11280		92,9	1,0
	200	6,93	15210		125,3	1,0
30	50	1,67	3206	–14	84,1	2,785
	100	3,39	6508		170,7	2,622
	150	5,14	9868		258,9	2,787
	200	6,93	13300		349,1	2,786
40	50	1,67	2945	–21	101,2	3,351
	100	3,39	5978		205,4	3,155
	150	5,14	9065		311,4	3,352
	200	6,93	12220		419,9	3,351
50	50	1,67	2652	–26	113,4	3,755
	100	3,39	6193		265,0	4,071
	150	5,14	8162		349,2	3,759
	200	6,93	11000		470,9	3,758

arch support and axial forces in M20 bolts of SD clamps. Four numerical models for different variants of V25 profile notches were analysed, as described in section 3.1. (30 mm, 40 mm, 50 mm notches and without notch). The calculation was made for a support load causing a change in the radius of about 100 mm (uniform load on the V25 profile's flange with a normal direction).

It should be noted that, as in Section 3.1, this is a test value for the load, related to the inducing of a specific arch deformation and not to the direct impact of the rock mass on the support.

The developed model corresponded to a section quarter of a single shaft support's ring. On the planes of symmetry appropriate supports were adopted. The operation of the friction joint was modelled as a "non-penetration" type contact and three spring type yielding elements, which are responsible for the mutual displacement of the overlap elements and the operation of SD clamps.

The analysis adopted a linear material model for S480W steel (Young's modulus $E = 200$ GPa, Poisson's coefficient $\nu = 0.3$) [16]. The calculation model is shown in Figure 19.

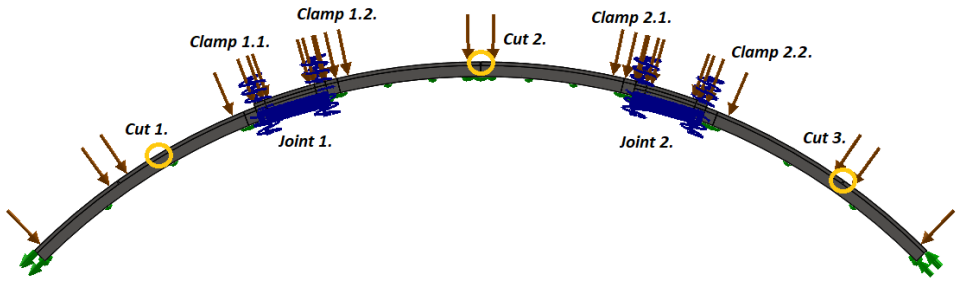

Fig. 19. Model of an arch support prepared for calculation

All models were identically supported and subjected to the same load. The calculations provided parameters such as the deformations and displacements of model elements, reduced stress values (according to the Huber-Misses hypothesis) and axial forces in elastic elements simulating friction joints. The results obtained were used to determine the effect of the section notches on the reduced stress in the cross-section of the V25 profile and the forces in the elements simulating the M20 bolts of SD clamps. Figures 20 and 21 show stress distributions and displacements in the models. The results of the analyses are presented in Table 2.

TABLE 2

Results of numerical analyses

Notch depth [mm]	Increase in force in M20 bolt of SD clamp [kN]				Max. stress in cross-section (von Mises) [MPa]		Friction joint axial force [kN]	Radius change [mm]
	Clamp 1.1.	Clamp 1.2.	Clamp 2.1.	Clamp 2.2.	Notch 1 and 3	Notch 2		
0	3.03	4.90	4.99	3.31	68	114	160	98
30	2.97	4.79	4.90	3.24	407	119		
40	2.83	4.69	4.80	3.17	528	122		
50	2.73	4.53	4.64	3.07	633	123		

The results show that making a notch in the V25 profile, depending on its depth, reduces the value of the force in the M20 bolts from 2% (at the 30 mm notch) to 10% (at the 50 mm notch). At the same time, the reduced stress values of the profile's cross section (for notch 1 and 3 more than nine times) increase. In the case of notch 2, the stress increase is insignificant (up to 8%). The 40 and 50 mm deep notch of the section involves local plasticisation of the material (for S480W

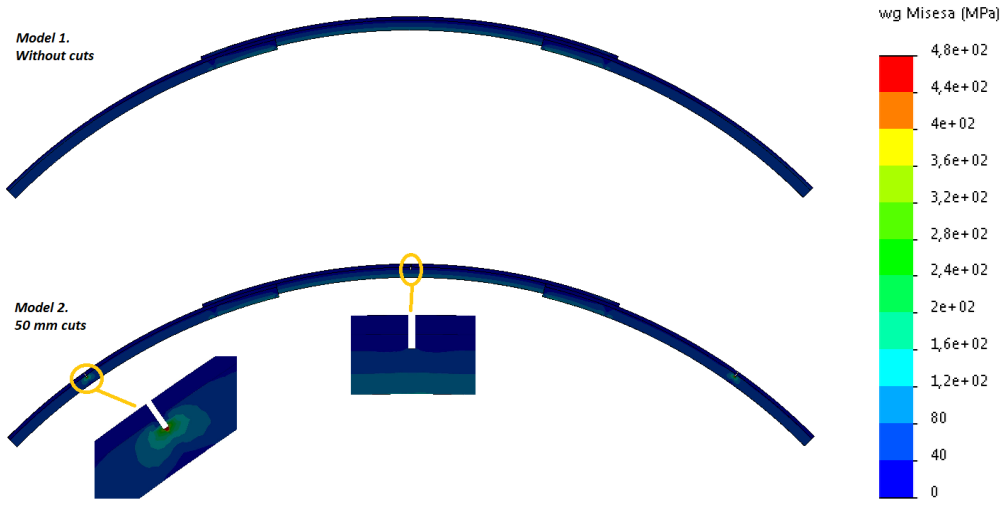

Fig. 20. Reduced stress distribution in the support model without notches and with a 50 mm notch, for deformation corresponding to a reduction of the radius of about 100 mm (stresses in MPa, actual scale of deformation)

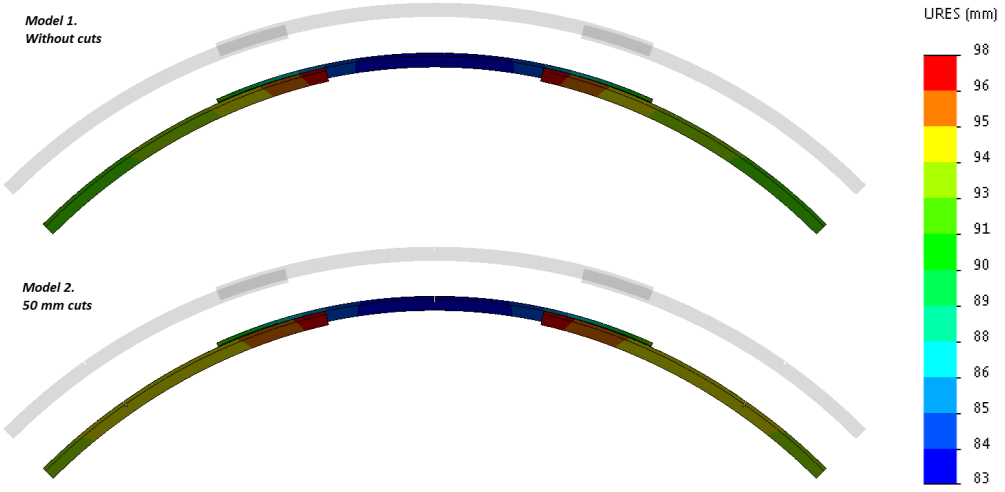

Fig. 21. Resultant displacement in the support model without notches and with a 50 mm notch, for deformation corresponding to a reduction of the radius of about 100 mm (displacements in mm, deformation scale 5×)

steel). The difference in the strength of the notch areas depending on the mutual position of the sections („external“ or „internal“ position in relation to the shaft's axis) should be highlighted. This is related to the kinematics of the support system and to the different share of the individual components of internal forces depending on the position of the arch.

3.3. Numerical analysis of the bending of the frictional joint of circular arch support-notches on V25 profile bottom

The last stage of the analysis was based on the numerical model created as described in Section 2.2. of the paper. The key difference was the change of the location of the V25 profile notches. This stage of calculation assumed notches in the bottom of the section. One numerical model was analysed for the 25 mm deep notch variant. The other conditions, including the support and strain distribution, as well as the representation of the slides in the frictional joint, are left unchanged from point 3.2. Figure 22 shows the reduced stress distribution and Figure 23 shows the model displacements. The results of the analyses are presented in Table 3.

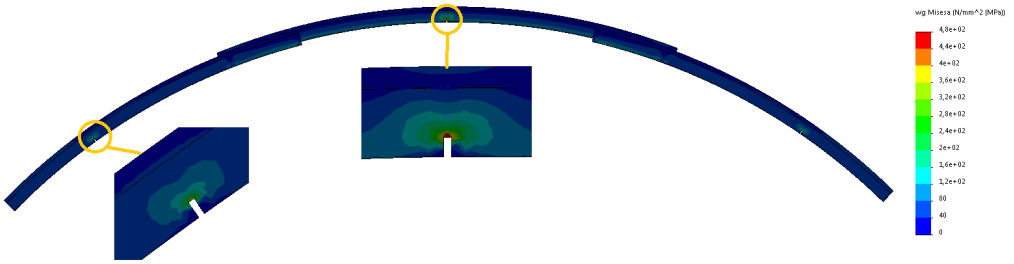

Fig. 22. Reduced stress distribution in the support model with a notch at the bottom of the V25 profile (25 mm deep), for deformation corresponding to a reduction of the radius of about 100 mm (stresses in MPa, actual scale of deformation)

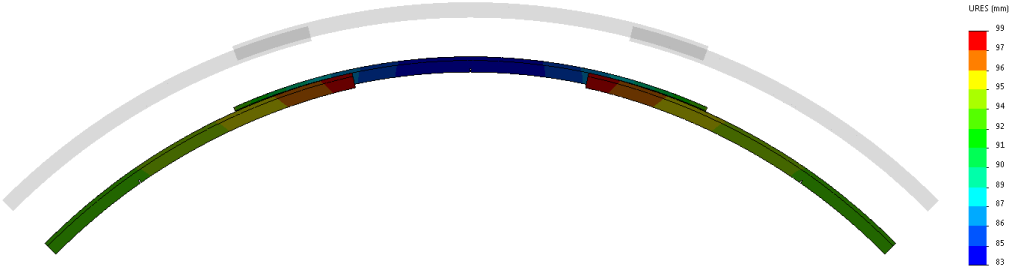

Fig. 23. Resultant displacements in the support model with a notch at the bottom of the V25 profile (25 mm deep), for deformation corresponding to a reduction of the radius by about 100 mm (displacements in mm, deformation scale 5×)

TABLE 3

Results of numerical analyses

Notch depth [mm]	Increase in force in the M20 bolt of the SD clamp, [kN]				Max. stress in cross-section (von Mises), [MPa]		Friction joint axial force [kN]	Radius change [mm]
	Clamp 1.1.	Clamp 1.2.	Clamp 2.1.	Clamp 2.2.	Notch 1 and 3	Notch 2		
0	3.03	4.90	4.99	3.31	68	114	160	98
25	3.21	5.25	5.36	3.48	382	615		

The analysis of the calculation results shows that making a 25 mm deep notch in the bottom of the V25 profile increases the force in M20 bolts by 6%. At the same time, the reduced stress values of the profile's cross section (for notch 1 and 3 more than five times) increase. However, in the area of the bottom of the notch these are compressive stresses.

4. Laboratory tests of V25 profiles

The bench tests of profiles with notches were carried out in the accredited Testing Laboratory for Mechanical Equipment at the Central Mining Institute. The tests were carried out on eight samples of the V25 profiles, in compliance with PN-G-15000-9:1998 standard [17]. A diagram of the test (support and load pattern of the section bars) is shown in Figure 24. The tested samples are listed in Table 4. The results provide the characteristics of individual samples. They are presented in Figure 25.

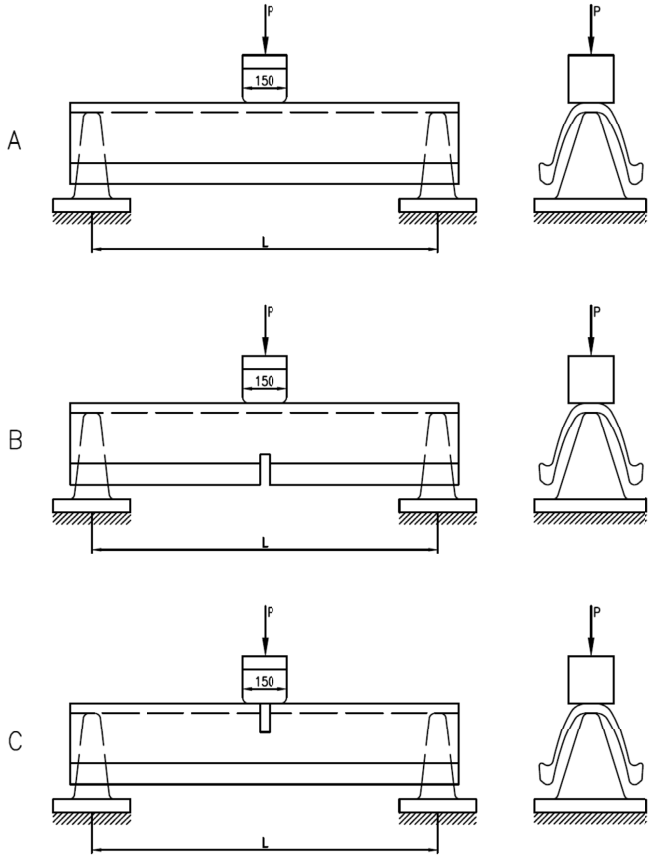

Fig. 24. Laboratory test scheme – static V profile bending test;
A – test of the sample without notches (tests 2.3), B – test of the sample with notched flange (tests 1,4,5,6,7), test of the sample with a bottom notch (test 8); P – load, L – support spacing (1.0 m)

TABLE 4

Characteristics of tested samples

Item	Symbols	Profile	Steel grade	Heat code	Rm	Re	Re/Rm	A	Notches
					MPa	MPa	—	%	—
1	19-94-1	V25	25G2	513598	386	577	0.67	30.8	One flange, 37 mm
2	19-94-2	V25	S480W	87023	572	703	0.81	26.0	No notches
3	19-94-3	V25	25G2	513603	409	614	0.67	31.5	No notches
4	19-94-4	V25	S480W	87043	575	730	0.79	24.1	Flanges, 36.6 and 36.4 mm
5	19-94-5	V25	S480W	87043	575	730	0.79	24.1	Flanges, 44.0 and 45.0 mm
6	19-94-6	V25	25G2	513598	386	577	0.67	30.8	Flanges, 41.1 and 41.6 mm
7	19-94-7	V25	25G2	513603	409	614	0.67	31.5	Flanges, 34.8 and 34.4 mm
8	19-94-8	V25	S480W	87023	572	703	0.81	26.0	Bottom, 24.0 and 23.4 mm

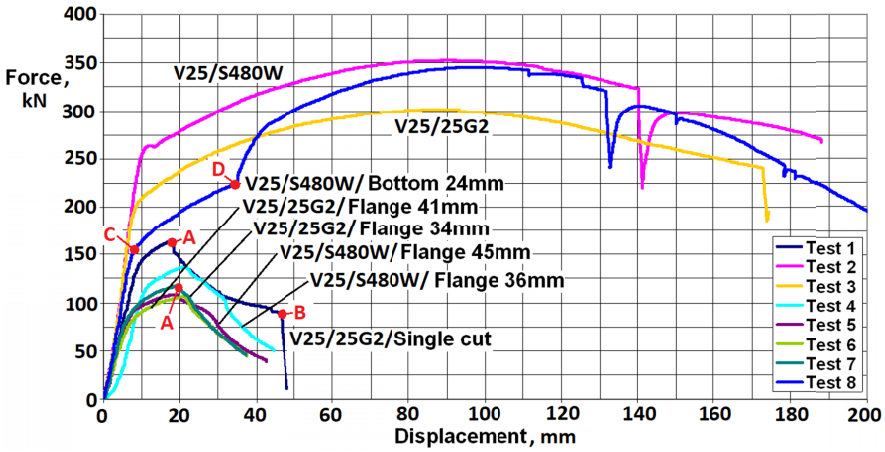

Fig. 25. Diagrams of the static bending test of the V25 profile

The graphs show, in the tests according to the scheme presented earlier, sections with notched flanges (tests 4-7) are characterized by a more than 50% decrease in load capacity compared to sections without notches (tests 2 and 3). The damage mechanism is alarming. All sections with notched flanges cracked when the maximum load was reached (point A in the diagram). Slightly earlier (the less inclined section of the graph) thickness reduction of the wall was noticed, analogous to the "neck" during the tensile test. At the time of the fracture, the load-bearing capacity of the samples dropped drastically, and the fracture propagated towards the bottom (Fig. 27). In case of test 1 (V-profile with single notched flange), however, the tests were carried out outside the deformation range provided in the standard. At the moment marked as B in the diagram, there was a fracture in the bottom and a sudden drop in the load capacity of the sample, practically to zero.

The last test on a section with a bottom with notches was interesting. When the load causing permanent deformation is reached, the characteristic reduces the slope (point C). The notch gap is then clearly closed. When it is completely closed, the section is stiffened (point D) and

its load-bearing capacity approaches the section without a notch. Such yielding method by the depth of notches allows the initial stiffness of the section to be adjusted (before closing the gap). By changing the notch width (in the tested sample ~4 mm), however, the position of point D of the re-stiffening of the section can be controlled on the section characteristics. Figure 28 shows the gap during closing.

Fig. 27. Section fracture during the test (sample 4)

Fig. 28. Closing the notch gap during the test

5. Determining the optimum notch depth of the V25 profile and assessing the impact of notches on the load-bearing capacity of the support

The analysis of the course and results of bench tests and numerical analyses indicate that the notches of the section flanges adversely affect the operation of the arch and the entire arch support. This results in a build-up of stress in the area of the bottom of the notch and, as a consequence, a fracture in the side walls of the section combined with a decrease in the load capacity of the block. Uncontrolled damage to the section – interruption of material continuity – practically excludes this solution as an additional (apart from frictional connectors) reinforcement of the support. Consequently, the notch can be applied only to the section bottom. This reduces the stiffness of the arch in the first bending phase and, depending on the width of the joint, stiffens the arch when the joint is closed. Therefore, a 4-5 mm wide notch of the bottom to a depth of 25-30 mm was proposed.

6. Alternative yielding methods

The circular arch support operates in conditions of considerable deformation, therefore, some alternative solutions in terms of notches aimed at increasing the yielding capacity of the arch support may be useful. Articulated arch cylindrical joints would reduce the diameter of the arch support without generating any additional stress due to the clamping of the arches. However, there is a serious risk, especially when multiple joints occur as a result of the splitting the arch support into elements. Another solution is the use of a mixed support in which the arches are made of different types of materials with different mechanical parameters.

Friction joints are quite a promising solution when equipped with one or two reinforced clamps built at the end of the overlap, as shown in Figure 29. At the same time, the scale construction of arches would unify the operation of all connections in the support. Increasing yielding capacity can be achieved by anchoring [21] of the arch support (rings) through "stringer-spreader" accessories. This solution is shown in Figure 30.

Another way to increase the yielding capacity of the circular arch support can be to bend the arches so that the radius of the curvature is much smaller than the diameter of the support.

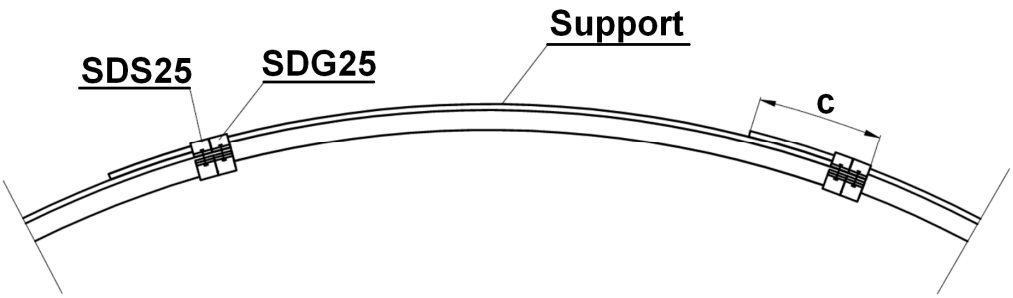

Fig. 29. Scale connection using friction joints with reduced load capacity

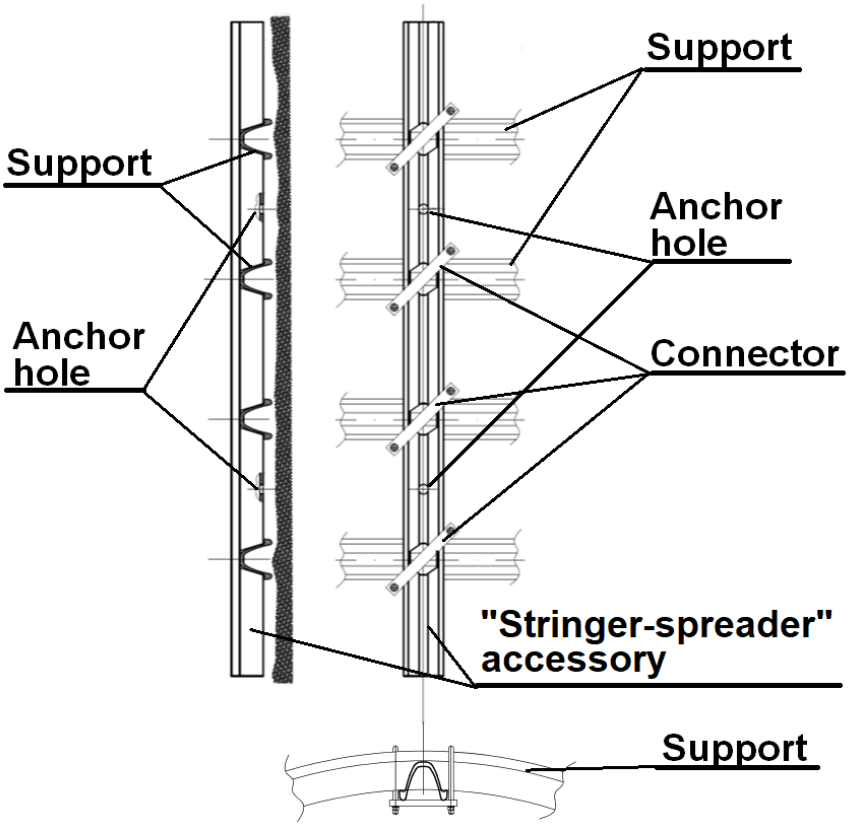

Fig. 30. Anchoring of the circular arch support by means of a spreader beam

Arches during their installation in the shaft would have to be pre-tensioned in terms of elastic deformation to match the diameter of the shaft. In such a case, the occurrence of the slide of the support would only be related to the load capacity of the friction joints and not to the deformation of the arches.

7. Conclusion

This work analysed the operation of circular arch support and some alternative methods (apart from the friction joint) to increase yielding capacity of arches in arch support. This requirement results from the observations made in the shaft located in an area of the deposit where there is a thick layer of rock salt. In this location the highest speed of the creep of the salt sidewall slightly exceeded 11.0 mm/day was observed.

The numerical analysis shows that notches in the flanges of the sections reduce the load impacting on the clamp's bolts (by about 10%), but lead to stress accumulation around the bottom of the notch (up to 9,3 times higher stress for maximum depth of notch).

In the laboratory tests, notches affected the damage mechanism of the V-profile element. Arches with notches are characterized by much smaller force causing damage. This difference reaches up to 60% (for probes with notched flanges). The nature of the damage to the sections disqualifies this solution as an additional method to increase yielding capacity. The bottom notch, however, does not reduce the load on the clamp's bolts, but allows the arch characteristics to be adapted to requirements of increased yielding capacity. Another good solution may be reinforced clamps (one or two) only at one end of the overlap, as described in section 6.

References

[1] G.G. Litwinskij, G.I. Gajko, N.I. Kyldyrkajew, *Stalnyje ramnyje kriepi gornych wyrabotok*. Kijew „Technika" (1999).

[2] G.I. Gayko G.I., M. Rotkegel, *Issliedowanija niesuszcziej sposobnosti arocznoj kriepi pri razlicznych wariantach nagrużienia*. Ugoł Ukrainy **2**, 45-47 (2003).

[3] M. Grodzicki, M. Rotkegel, *The concept of modification and analysis of the strength of steel roadway supports for coal mines in the Soma Basin in Turkey*. Studia geotechnica et mechanica **1**, 38-45 (2018).

[4] L.V. Cong, Nghiên cứu thiết kế vì chống thép phục vụ chống giữ các đường lò tiết diện lớn bằng thép V (có mô men chống uốn cao) trong các mỏ hầm lò vùng Quảng Ninh. Project summary. Ministry of Science and Technology. Hanoi. Vietnam (2016).

[5] T.T Minh, D.Q. Tuan, N.N. Bay, *Research on the state of stress-deformation in rock mass and assessment effects of supports around roadways in underground mines* (in Vietnamese: Nghiên Cứu Trạng Thái Ứng Suất-Biến Dạng Trong Khối Đá Và Đánh Giá Hiệu Quả Của Kết Cấu Chống Giữ Xung Quanh Các Đường Lò). University of Mining and Geology. Hanoi. Vietnam (2016).

[6] T.M. Tran, P. Nguyen, T. Nguyen, *Technique and Technology of underground construction in mining* (in Vietnamese: Kỹ thuật và công nghệ xây dựng công trình ngầm trong mỏ). Nha xuat ban xay dung. Hanoi. Vietnam (2016).

[7] W. Korzeniowski, D. Terpak, *Podziemna eksploatacja lignitu systemem ścianowym podbierkowym w kopalniach HBP Prievidza na Słowacji*. Przegląd Górniczy **10**/2014 (2014).

[8] PN-H-93441-3 - Kształtowniki stalowe walcowane na gorąco dla górnictwa. Kształtowniki typu V. Wymiary.

[9] PN-H-84042 - Stale mikrostopowe na kształtowniki i akcesoria górnicze.

[10] R.D. Cook, D.S. Malkus, M.E. Plesha, R.J. Witt, *Concepts and applications of finite element analysis*. John Wiley & Sons, Inc. USA (2002).

[11] T. Chmielewski, H. Nowak, *Mechanika budowli. Metoda przemieszczeń. Metoda Crossa. Metoda elementów skończonych*. Wydawnictwa Naukowo-Techniczne, Warszawa (1996).

[12] COSMOS/M v 2.5. *User's Guide*. Structural Research & Analysis Corporation (1999).

[13] E. Rusiński, *Metoda elementów skończonych. System COSMOS/M*. Wydawnictwo Komunikacji i Łączności, Warszawa (1994).

[14] M. Rotkegel, *Komputerowo wspomagane projektowanie odrzwi obudowy chodnikowej. Charakterystyka programu CAD i przykłady projektowe*. Prace Naukowe GIG. Nr 862. Katowice (2004).

[15] M. Rotkegel, *Program komputerowy do wspomagania konstruowania odrzwi stalowej obudowy wyrobisk korytarzowych*. Wiadomości Górnicze **12**/2009. Katowice, 2009.

[16] Ł. Szot, *Modele materiałowe wybranych gatunków stali stosowanych na odrzwia obudowy wyrobisk korytarzowych*. Przegląd Górniczy **7**/2016. SiTG (2016).

[17] PN-H-15000-09 - Obudowa chodników odrzwiami podatnymi z kształtowników korytkowych. Kształtowniki korytkowe proste. Próba statyczna zginania.

[18] G. Walton, E. Kim, S. Sinha, G. Sturgis, D. Berberick, *Investigation of shaft stability and anisotropic deformation in a deep shaft in Idaho, United States*. International Journal of Rock Mechanics and Mining Sciences **105**, 160-171 (2018).

[19] J. Stasica, Z. Rak, Z. Burtan, *Nowoczesne technologie napraw i wzmocnień obudowy szybów górniczych*. Zeszyty Naukowe Instytutu Gospodarki Surowcami Mineralnymi i Energią Polskiej Akademii Nauk **101**, 133-146 (2017).

[20] J. Stasica, *Nowoczesne metody badań i oceny stanu technicznego obudów szybów górniczych*. Zeszyty Naukowe Instytutu Gospodarki Surowcami Mineralnymi i Energią Polskiej Akademii Nauk **101**, 85-100 (2017).

[21] T. Majcherczyk, Z. Niedbalski, P. Małkowski, Ł. Bednarek, *Analysis Of Yielding Steelarch Support With Rock Bolts In Mine Roadways Stability Aspect*. Archieves of Mining Science **59**, 3, 641-654 (2014).

[22] S. Fabich, J. Bauer, M. Rajczakowska, S. Świtoń, *Design Of The Shaft Lining And Shaft Stations For Deep Polymetallic Ore Deposits: Victoria Mine Case Study*. Mining Science **22**, 127-146 (2015).